

Serveur Académique Lausannois SERVAL serval.unil.ch

Author Manuscript

Faculty of Biology and Medicine Publication

This paper has been peer-reviewed but does not include the final publisher proof-corrections or journal pagination.

Published in final edited form as:

Title: Molecular and therapeutic characterization of anti-ectodysplasin A receptor (EDAR) agonist monoclonal antibodies.

Authors: Kowalczyk C, Dunkel N, Willen L, Casal ML, Mauldin EA, Gaide O, Tardivel A, Badic G, Etter AL, Favre M, Jefferson DM, Headon DJ, Demotz S, Schneider P

Journal: The Journal of biological chemistry

Year: 2011 Sep 2

Volume: 286

Issue: 35

Pages: 30769-79

DOI: 10.1074/jbc.M111.267997

In the absence of a copyright statement, users should assume that standard copyright protection applies, unless the article contains an explicit statement to the contrary. In case of doubt, contact the journal publisher to verify the copyright status of an article.

MOLECULAR AND THERAPEUTIC CHARACTERIZATION OF ANTI-ECTODYSPLASIN A RECEPTOR (EDAR) AGONIST MONOCLONAL ANTIBODIES.

Christine Kowalczyk^{1,9}, Nathalie Dunkel^{1,9,10}, Laure Willen¹, Margret L. Casal², Elizabeth A. Mauldin², Olivier Gaide³, Aubry Tardivel¹, Giovanna Badic^{1,10}, Anne-Lise Etter^{4,10}, Manuel Favre^{4,10}, Douglas M. Jefferson^{5,6}, Denis J. Headon⁷, Stéphane Demotz^{8,10} and Pascal Schneider¹
¹Department of Biochemistry, University of Lausanne, CH-1066 Epalinges, Switzerland. ²School of Veterinary Medicine, University of Pennsylvania, Philadelphia 19104-6010, USA. ³Department of Dermatology, University of Geneva, CH-1211 Geneva, Switzerland. ⁴Apoxis SA, CH-1004 Lausanne, Switzerland. ⁵Cell Essential, 198 Tremont Street, Boston MA02116, USA. ⁶Tufts University School of Medicine, Boston MA 02111, USA. ⁷Roslin Institute and Royal (Dick) School of Veterinary Studies, University of Edinburgh, Roslin EH25 9PS, UK. ⁸Edimer Biotech, Ch de l'Eglise 7, CH-1066 Epalinges, Switzerland. ⁹Contributed equally to the work. ¹⁰Present addresses: ND: Department of Oncology, Geneva University Hospital, CH-1211 Geneva. SD: Philip Morris Products SA, CH-2000 Neuchâtel. GB: Instrumat AG, Rueyre 116, CH-1020 Renens, Switzerland. ALE: Celgene International, CH-2074 Marin. MF: Merck-Serono, CH-1809 Fenil-sur-Corsier, Switzerland.

Running title: agonist anti-EDAR antibodies.

Abbreviations: EDA: Ectodysplasin A. EDAR: EDA Receptor; GPI: glycosyl-phosphatidylinositol.

Address correspondance to: Pascal Schneider, Department of Biochemistry, University of Lausanne, Boveresses 155, CH-1066 EPALINGES, Switzerland; Phone: +41 21 692 5709; Fax:+41 21 692 5705; E-mail: pascal.schneider@unil.ch

The TNF family ligand ectodysplasin A (EDA) and its receptor EDAR are required for proper development of skin appendages such as hair, teeth and eccrine sweat glands. Loss of function mutations in the *Eda* gene cause X-linked hypohidrotic ectodermal dysplasia (XLHED), a condition that can be ameliorated in mice and dogs by timely administration of recombinant EDA. In this study, several agonist anti-EDAR monoclonal antibodies were generated that cross-react with the extracellular domains of human, dog, rat, mouse and chicken EDAR. Their half-life in adult mice was about 11 days. They induced tail hair and sweat gland formation when administered to newborn EDA-deficient *Tabby* mice, with EC₅₀ of 0.1 to 0.7 mg/kg. Divalency was necessary and sufficient for this therapeutic activity. Only some antibodies were also agonists in an *in vitro* surrogate activity assay based on the activation of the apoptotic Fas pathway. Activity in this assay correlated with small dissociation

constants. When administered *in utero* in mice or at birth in dogs, agonist antibodies reverted several ectodermal dysplasia features, including tooth morphology. These antibodies are therefore predicted to efficiently trigger EDAR signaling in many vertebrate species and will be particularly suited for long-term treatments.

The TNF family comprises 19 ligands, most of which control development, function and/or homeostasis of the immune system (1). In this respect, Ectodysplasin A (EDA) is an exception as it participates in ectodermal appendage formation (2). The *Eda* gene on the X chromosome is transcribed as multiple splice variants, only two of which code for the receptor-binding C-terminal TNF homology domain. These two variants, generated by splicing at an alternative donor sites between exons 8 and 9, code for 391 and 389 amino acid-long proteins called EDA1 and EDA2 (3). EDA1 binds the receptor EDAR, whereas EDA2 binds to another receptor, XEDAR (3). The

biology of EDA2 and XEDAR is distinct from that of EDA1. Indeed, XEDAR-deficient mice have no obvious ectodermal dysplasia phenotype, whereas mice deficient in EDA, EDAR or the signaling adaptor protein EDARADD, all display virtually indistinguishable ectodermal dysplasia phenotypes, indicating the predominance of the EDA1 – EDAR axis in the development of skin-derived appendages (4-8).

In human, EDA1 loss of function mutations cause X-linked hypohidrotic ectodermal dysplasia (XLHED), a rare condition characterized by defective formation of teeth, hair, sweat glands and other glands (6). Because of their insufficient number of sweat glands, these patients are prone to hyperthermia. They also frequently suffer from recurrent respiratory tract infections caused by abnormal mucus production in the airways. Other problems are oligodontia, dry skin and dry eyes (9-11).

EDA1 is a transmembrane Type II protein with a furin consensus cleavage site, a collagen-like domain and a C-terminal TNF homology domain, any of which when mutated can cause XLHED (12). In order to be active, EDA must be processed and bind EDAR through its trimeric C-terminal domain. The signaling ability of EDA1 is reinforced by its collagen domain that cross-links individual EDA1 trimers (13). Interestingly, some EDA1 mutations can also cause selective tooth agenesis, a condition characterized by no or very little involvement of other ectodermal appendages (14). In these patients, EDA1 mutants retain partial binding to EDAR, suggesting that tooth development is particularly sensitive to “high quality” EDAR signals.

Transgenic expression of EDA1 in skin under the keratin 14 promoter results in a disheveled hair phenotype, hypertrophy of sebaceous glands and formation of supernumerary molars or nipples (15). Transgenic EDA1 expression in the skin of EDA-deficient *Tabby* mice corrected many of the ectodermal dysplasia defects (16). The reverted phenotype was stable even after shutdown of transgenic EDA1 expression in young adults, suggesting that EDA1 plays a role in the formation but not in the maintenance of skin appendages. Interruption of EDA1 expression however resulted in the normalization of sebaceous gland size (16). Similar conclusions were reached with an alternative approach of protein replacement

therapy, in which EDA-deficient animals were exposed to a recombinant form of EDA during development (17,18). Taken together, these data provide a proof of concept for protein replacement therapy in young patients with XLHED.

In this study, we generated agonist anti-EDAR antibodies that mimic the action of transgenic or recombinant EDA1 in development. Most of these antibodies cross-react with EDAR of mammals and birds and are active as monomeric, divalent molecules. They corrected, among others, sweat glands, tracheal glands and tooth morphology in EDA-deficient mice and were also active in EDA-deficient dogs. These mouse monoclonal antibodies will be reagents of choice for long-term experiments in mice and pave the way for the development of therapeutic antibodies for use in XLHED or other EDAR-related applications in humans.

EXPERIMENTAL PROCEDURES

Animals - Mice were handled according to Swiss Federal Veterinary Office guidelines, under the authorization of the Office vétérinaire cantonal du canton de Vaud (authorization 1370.3 to PS). White-bellied agouti B6CBAa $A^{w-J}/A-Eda^{Ta}/J$ *Tabby* mice (000314; Jackson Laboratory) were bred as Eda^{Ta}/Eda^{Ta} and Eda^{Ta}/Y mutants, or as $+/+$ and $+/Y$ wild type controls. EDAR-deficient OVE1B mice were as described (5). EDA-deficient dogs (19) were cared for in accordance with the principles outlined in the National Institutes of Health Guide for the Care and Use of Laboratory Animals and in the International Guiding Principles for Biomedical Research Involving Animals.

Plasmids and recombinant proteins - Plasmids used in this study were either previously published, or derived from the published plasmids by standard molecular biology techniques (13,20,21) (Fig. S1). A fully human form of Fc-EDA1 was kindly provided by Dr Neil Kirby (EdimerPharma, Boston). hEDAR-Fc and mEDAR-Fc were produced and purified as described (21).

Generation and purification of anti-EDAR monoclonal antibodies - 150 μ g of hEDAR-Fc or mEDAR-Fc (amino acid residues 29-183. Fig. S1)

were briefly sonicated three times in 750 μ l of PBS:STIMUNE (1:1, v/v) (Cedi-diagnostics, Lelystad, The Netherlands). Female OVE1B mice were immunized subcutaneously (base of tail, 200 μ l) with the antigen preparation, and boosted between days 10 to 14 with antigen in PBS:STIMUNE (base of tail, 150 μ l). Mice positive for anti-EDAR antibodies at day 30 were boosted with 150 μ g antigen in PBS at day 40 (base of tail). Three days later, lymph node cells were fused with myeloma cells according to standard procedures, grown in complete RPMI medium over a feeder layer of mouse macrophages, and selected 24 h later with HAT (hypoxanthine, aminopterin and thymidine)-containing medium. Supernatants of 96 wells plates were tested by ELISA for antibody secretion. Positive clones were subcloned twice by limiting dilution, and then slowly adapted to medium without macrophages and HAT supplement. Most hybridoma could then be progressively adapted to serum-free Opti-MEM medium (Invitrogen). Antibodies were purified from conditioned Opti-MEM supernatants by affinity chromatography on Protein G-Sepharose (GE Healthcare).

Transfections - HEK 293T cells were grown in DMEM, 10% fetal calf serum and transfected by the calcium phosphate method. Cells were grown for 7 days in serum-free Opti-MEM medium (Invitrogen) for the production of EDAR-Fc truncation mutant fusion proteins, or for 48 h in complete medium for surface expression of receptors:TRAILR3 fusion proteins.

ELISA - For the detection of anti-EDAR antibodies, ELISA plates were coated with hEDAR-Fc at 1 μ g/ml, blocked and revealed with anti-EDAR antibodies (adequately diluted serum of EDAR immunized mice, hybridoma supernatants or purified antibody) followed by a peroxidase-coupled goat anti-mouse IgG (Jackson Immunoresearch). For isotype determination, ELISA plates were coated with 1 μ g/ml of anti-EDAR antibodies and revealed with peroxidase-coupled antibodies against the heavy chain of mouse IgG1, IgG2a or IgG2b (SouthernBiotech). For epitope mapping, ELISA plates were coated with an Fab₂ fragment of a goat anti-human Ig (Jackson Immunoresearch) to capture various

EDAR-Fc constructs or BCMA-Fc in cell supernatants. EDAR-Fc constructs and BCMA-Fc were revealed either with peroxidase-coupled donkey anti-human (H+L) (Jackson Immunoresearch), or with anti-EDAR antibodies at 1 μ g/ml followed by peroxidase-coupled goat anti-mouse IgG (Jackson Immunoresearch), or with Flag-EDA1 or Flag-BAFF followed by biotinylated anti-Flag M2 antibody (Sigma) and peroxidase-coupled streptavidin.

SDS-PAGE, Western blot, and native gel electrophoresis - Anti-EDAR antibodies (10 μ g/lane) were analyzed by SDS-PAGE under reducing conditions followed by Coomassie blue staining. Antibodies were also analyzed by native gel electrophoresis (4 μ g/lane) (Biomidi, Toulouse, France) and stained with amidoblack according to manufacturer's instructions, except that the electrophoresis was performed for 1 h.

To test the ability of anti-EDAR antibodies to recognize denatured EDAR, 2 μ g of bovine serum albumin, 20 ng of hEDAR-Fc and 20 ng of hFas-Fc were analyzed by SDS-PAGE and western blot under reducing (100 mM dithiothreitol) or non-reducing conditions, revealed with the various anti-EDAR antibodies at 1 μ g/ml followed by peroxidase-coupled anti-mouse antibody (1:10000) and ECL reagent (GE Healthcare).

Sequencing of anti-EDAR antibodies - RNA was extracted from hybridoma cells with an RNAeasy kit (Qiagen) according to manufacturer's guidelines. cDNA was prepared by reverse transcription with Ready-To-Go T-Primed First-Strand Kit (GE Healthcare). Variable sequences of the heavy and light chains were amplified by PCR as described (22). PCR products were sequenced on both strands. Sequences were analyzed for gene usage using the IMGT sequence alignment software (<http://imgt.cines.fr/>).

FACS analyses - 293T cells co-transfected with EGFP and receptor-GPI expression plasmids were stained with Fc-EDA1 or Fc-EDA2 essentially as described before (20), or with anti-EDAR antibodies at 4 μ g/ml followed by PE-coupled anti-mouse secondary antibody. Following staining, cells were analyzed using a FACScan flow cytometer (BectonDickinson) and FlowJo software (TreeStar, Ashland, OR).

Fab generation and affinity determination by surface plasmon resonance - An IgG1 Fab and Fab'2 preparation kit was used according to manufacturer's instructions (Pierce). Briefly, purified anti-EDAR antibodies were digested for 72 h at 37°C with immobilized ficin. Fc fragments and undigested antibodies were removed by chromatography on Protein A. The flow through, containing the Fab and Fab'2 fragments, was concentrated and applied onto a Superdex-200 gel permeation chromatography column eluted in PBS. Absorbance was recorded at 280 nm.

For surface plasmon resonance, human EDAR-Fc was captured on anti-human IgG Fc-derivatized CM5 chips in a Biacore T100 (GE Healthcare). Fab solutions of anti-EDAR antibodies at the indicated concentration in PBS were applied for 90 sec at 50 µl/min, and subsequently washed with buffer. All curve fittings were performed assuming a 1:1 binding model, although 2 antibodies had a biphasic dissociation that did not fit the 1:1 model.

In vitro cytotoxicity assays - Fas-deficient hEDAR:Fas Jurkat cells have been described before, and mEDAR:Fas expressing cells were obtained by retroviral infection according to the same protocol (13). The cytotoxicity assay using EDAR:Fas Jurkat cells was performed as described for FasL on Jurkat cells (23).

Injections in EDA-deficient animals - *Tabby* pups were labeled by puncture of a footpad with a 30-gauge needle dipped in china ink. Intraperitoneal injections with anti-EDAR antibodies or Fc-EDA1 were performed within 24 h after birth with a maximal volume of 15 µl, using 0.5 ml U-100 insulin syringes (Becton Dickinson). Examination and photography of tail hairs were performed at days 20 to 22 post-injection. Pregnant *Tabby* mice were treated iv at days 13 and 20 (E13/E20) or 9 and 17 (E9/E17) of gestation with 400 µg of anti-EDAR antibody (antibody 3). Offspring were analyzed at 6 months of age, essentially as described (18). Age-matched wild-type and EDA-deficient *Tabby* mice were similarly analyzed for comparison. Tracheal glands were detected by Alcian blue staining (24). Three dogs affected with X-linked ectodermal dysplasia were administered agonist anti-EDAR antibody 3 in the jugular vein at two days of live (n=2; 10 mg/kg) or at 14 days

of live (n=1; 7 mg/kg). The analysis was performed essentially as described (17,25). In particular, the dogs were monitored daily for adverse reactions, overall health, and specific ocular and respiratory diseases. Complete blood cell counts and serum biochemistry screens were evaluated within 2 to 7 days after injection with agonist anti-EDAR antibody. Dental radiographs were obtained when the dogs were adults, when about one year old. Shirmer tear testing was performed at 6-month intervals. Complete necropsies were performed between 1.6 and 2.4 years of age. Tissues were fixed in 10% neutral buffered formalin, routinely processed, sectioned at 5 µm and stained with hematoxylin and eosin.

RESULTS

Generation and screening of agonist anti-EDAR antibodies - To obtain cross-reacting antibodies against conserved EDAR regions, EDAR-deficient mice were immunized with either human or mouse EDAR-Fc fusion proteins. The EDAR-deficient mouse strains *Downless* and *Sleek* have loss-of-function mutations in the extracellular or intracellular domains of EDAR, respectively, but still express the protein. We therefore immunized OVE1B mice in which the *Edar* gene is completely deleted by random genomic integration of an unrelated transgene (5,26). Hybridoma supernatants with anti-EDAR reactivity were screened for agonist activity using two complementary tests. In the first one, surrogate reporter cell lines stably expressing hEDAR:Fas or mEDAR:Fas fusion proteins were used. EDAR activation in these reporter cells leads to apoptotic cell death by activation of the Fas pathway (13). In the second assay, hybridoma supernatants were administered intra-peritoneally to newborn, EDA-deficient *Tabby* pups (18). *Tabby* mice completely lack tail hairs, and the agonist activity of antibodies can therefore be measured by the induction of tail hair, provided that antibodies recognize and activate mouse EDAR. Several hybridoma secreted agonist antibodies with *in vivo* activity, but only few were also active in the cell-based *in vitro* assay (data not shown). Selected hybridoma were subcloned and adapted for growth in serum-free medium from which antibodies were purified (Fig. 1A). The monoclonal nature of these

antibodies was further confirmed by their sharp migration in native protein electrophoresis (Fig. 1B).

Agonist anti-EDAR antibodies have varied but relatively limited sequence characteristics - Variable regions of heavy and light antibody chains were amplified by RT-PCR and sequenced for several hybridoma. A number of different variable region genes were identified for both the heavy and light chains (Table 1), but some of them were shared by two or three hybridoma, usually with different somatic mutations. Interestingly, antibodies with identical heavy and light variable genes sharing greater than 90% sequence identity were obtained from different mice immunized with mouse (antibody 8) or human EDAR (antibodies 1 and 3) (Table 1, Fig. S2). Thus, different variable genes can be used to generate agonist anti-EDAR antibodies, but the gene repertoire must be limited as similar antibodies were found two or three times in the relatively limited panel that we have analyzed.

Agonist antibodies recognize at least three different epitopes in EDAR - EDAR contains three cysteine-rich domains (CRD) in its extracellular region, plus a stalk sequence (Fig. 2A). We used EDAR constructs containing these four regions alone or in combinations to roughly characterize the epitopes recognized by the antibodies. Some antibodies recognized CRD1 alone, others recognized CRD1 and 2 together and one reacted with CRD1, 2 and 3, but none bound to receptors lacking CRD1 (Fig. 2B, Table 1). All antibodies recognized recombinant EDAR by Western blot under non-reducing conditions, but only three reacted with reduced EDAR (Fig. 2C). These three antibodies had their epitopes localized in CRD1. It is possible that the presence of CRD1 is required for correct folding of EDAR. Abnormal disulfide bridge formation in the absence of CRD1 would explain why antibodies did not recognize constructs containing CRD2 and CRD3. Taken together, these results indicate that agonist anti-EDAR antibodies can recognize at least three different EDAR epitopes located in CRD1 and probably CRD2 and CRD3.

Agonist anti-EDAR antibodies cross-react with EDAR of various mammals and birds - Most anti-

EDAR antibodies cross-reacted with human, dog, rat, mouse and chicken EDAR when these were expressed as GPI-anchored molecules in 293T cells (Fig. 3). Antibody 5 only reacted minimally with chicken EDAR, whereas antibody 15 that had been selected on the basis of its specificity for human EDAR rather than for its agonist activity recognized human and dog EDAR, but not rat, mouse and chicken EDAR (Fig. 3).

Binding characteristics of anti-EDAR antibodies to EDAR - The affinity of eleven agonist antibodies to human EDAR was determined by surface plasmon resonance. For this purpose, monomeric Fab fragments were generated by ficin digestion and size exclusion chromatography (Fig. 4A). Affinities varied from 0.5 to 40 nM, and differences were also observed in the association and dissociation constants (Fig. 4B and Table 1). The dissociation kinetics of two antibodies (7 and 14) were biphasic, showing first a rapid dissociation followed by a slower dissociation, but as these antibodies had no remarkable agonist activity, this was not analyzed further.

Comparison of the activity of agonist anti-EDAR antibodies in vitro and in vivo - As we have not yet been able to identify a simple and quantitative assay to characterize EDAR agonists using EDAR's own signaling pathway *in vitro*, we used a surrogate reporter assay in which Fas-sensitive cells were transfected with the extracellular domain of human or mouse EDAR fused to the intracellular portion of Fas. Binding of an active recombinant EDA1 (Fc-EDA1) to these cells induces cell death by activation of the pro-apoptotic Fas pathway (13). Interestingly, only some of the antibodies (1, 3, 8, 10 and 12) (Fig. 5A) killed mEDAR:Fas expressing cells, and even fewer killed hEDAR:Fas expressing cells (1, 3, 10 and 12) (Fig. 5B, Table 1). In all cases, antibodies were less active than Fc-EDA1 by one to two orders of magnitude. The picture was different in an *in vivo* assay, where newborn *Tabby* mice were treated with antibodies on the day of birth. In this case, all antibodies rescued tail hair formation in a dose-dependent manner and with similar EC₅₀ of 0.1 to 0.7 mg/kg (Fig. 6). Only one of the antibodies (antibody 11) seemed less active, with an EC₅₀ of about 3 mg/kg. Functional sweat glands were induced by the treatment with similar

EC₅₀ as for tail hair (data not shown). The half-life of two antibodies (1 and 3) was determined in adult Tabby mice and found to be 10.5 and 11 days, respectively (Fig. S3).

Divalent monomeric agonist antibodies are active in vivo - We have shown previously that cross-linked EDA1 containing more than one trimer in a single molecule are better agonists than trimeric EDA1 (13). We therefore wondered whether the *in vivo* activity of agonist anti-EDAR antibodies was due to monomeric antibodies or to aggregates thereof. The activity of a monomeric (divalent) antibody purified by size exclusion chromatography (Fig. 6, antibody 1) was however very similar to that of the total preparation (data not shown), and compared favorably (EC₅₀ ~0.1 mg/kg) with recombinant Fc-EDA1 (EC₅₀ ~0.05 mg/kg) (Fig. 6). In addition, the Fab'₂ fragment, but not the Fab fragment, was active *in vivo* when administered in newborn pups on the day of birth (Fig. S4). When the Fab'₂ was administered later at day 3 post-birth, one of the latest time points where ventral tail hair can be induced, its action could be inhibited by an excess of the Fab fragment, ruling out that the lack of agonist activity of the Fab would be due only to a shorter half-life *in vivo* (Fig. S4). We conclude from these observations that a divalent agonist anti-EDAR antibody is both sufficient and necessary to exert activity in *Tabby* mice.

Effective treatment of EDA-deficient mice with agonist anti-EDAR antibodies - Some patients with partially inactivating EDA mutations have teeth defects but otherwise normal skin appendages, suggesting that tooth formation may require more stringent EDAR signals than other skin appendages for proper development (14). In order to test the effect of agonist antibodies on tooth development, pregnant *Tabby* mothers were treated during pregnancy so that the antibody could be transferred to embryos by the transplacental antibody transport system. Mice exposed to agonist anti-EDAR during development not only had tail hairs and functional sweat glands, but also hair behind the ears, mucus-secreting glands in the trachea and a normalized eye appearance (Fig. 7 A-G and Fig. S5). In addition molars of treated mice were reverted and almost indistinguishable from those of wild type animals

(Fig. 7 H-I, Fig. S5). The effect was long-lasting, as a similarly treated mouse was still reverted after more than 2 years (Fig. S6). Taken together, these results indicate that the two agonists anti-EDAR antibodies tested in this application (1 and 3, Fig. 7, S4 and data not shown) revert the ectodermal dysplasia phenotypes that we have looked at in *Tabby* mice, including tooth morphology.

Activity of agonist anti-EDAR antibodies in EDA-deficient dogs - Agonist anti-EDAR antibodies recognize EDAR of different species (Fig. 3). In order to test whether the observed cross-species reactivity also holds true for the agonist activity, anti-EDAR antibody 3 was administered intravenously to three EDA-deficient dogs at either 2 days of life (n=2, 10 mg/kg) or at 14 days of life (n=1, 7 mg/kg). None of these dogs showed adverse reactions upon injection. Dentition was corrected not only in EDA-deficient dogs that were treated at 2 days of life, but also in the affected treated at 14 days of life, although the latter still lacked premolars, accounting for the decreased number of teeth (Fig. 8 and Table 2). Interestingly, the premolars and molars in dogs treated at day 2 of life had a more normal appearance than in those dogs treated with Fc-EDA (17). Lacrymation was improved in treated dogs except in one treated at day two of age (Table 2). The correction of glands in trachea, bronchi and esophagus appeared however to be dependent on the age at which the dogs were treated: treatment administered earlier in life had a bigger impact on gland development (Fig. 8 and Table 2). It is noteworthy that, regardless of the extent of the phenotypic reversion, none of the treated dogs suffered from pneumonia or other airway diseases that are common in untreated EDA-deficient dogs, or from dry eye condition (keratoconjunctivitis sicca) that affect all XLHED dogs.

DISCUSSION

Deficiency in the TNF family ligand EDA leads to ectodermal dysplasia, even if the receptor EDAR remains fully functional. The development of EDAR agonists are thus of interest for applications in the treatment of XLHED. EDAR is relatively well conserved across species, with only 4 amino acid differences between human and dog, 10 between human and mouse and 13 between human

and chicken in the 154 amino acid residues-long mature extracellular domain (Fig. S7). In order to increase the likelihood of getting cross-reactive antibodies, EDAR-deficient mice were used to generate monoclonal antibodies. The approach proved successful as 13 of the 15 anti-EDAR antibodies analyzed recognized EDAR from human, dog, rat, mouse and chicken. These antibodies are therefore likely to cross-react with EDARs of all mammals and many other vertebrates. Anti-EDAR15 differentiated human and dog from rat and mouse EDARs whose primary sequence only diverge in CRD1 (Fig. S7), implying that part of its epitope is in CRD1. Anti-EDAR9 recognized CRD1, 2, and 3 of EDAR, but none of the CRDs taken individually or in pairs, despite the fact that these fragments were overlapping and supposed to respect structural elements of the receptor. These results indicate that EDAR may fold on itself to create a conformational epitope with regions that are distant in the primary sequence. In any case, results indicate that agonist anti-EDAR antibodies can recognize at least 3 distinct epitopes in EDAR.

Anti-EDAR antibodies were screened in newborn *Tabby* mice, a highly relevant *in vivo* assay whose main limitation is to detect only antibodies cross-reacting with mouse EDAR. More than half of the 46 hybridoma supernatants tested were active in this assay, indicating that agonist antibodies can readily be obtained with the procedure used. The success rate of detection was however lower using the EDAR:Fas reporter cell lines that signal cell death in an oligomerization-sensitive manner, probably because these cell-based assays make use of a different intracellular signaling pathway. When combined, these assays discriminated two classes of agonist anti-EDAR antibodies, with or without *in vitro* activity. Interestingly, the *in vitro* activity correlated relatively well with low antibody dissociation constants, but not with association constants or affinities (Fig. S8). The EDAR:Fas reporter cells were previously shown to discriminate recombinant WT EDA1 and EDA1 with the V365A mutation identified in a family with selective tooth agenesis, despite the fact that these two ligands bind EDAR-Fc almost equally well (14). This led to the hypothesis that formation of teeth may require higher quality EDAR signals than those needed for hair or gland formation.

Thus, it is possible that agonist antibodies with activity *in vitro* may also be the best ones to correct tooth defects associated with EDA-deficiency. It will be interesting to experimentally test this hypothesis in the future.

The plethora of anti-EDAR agonist antibodies obtained, most of which were of the IgG1 isotype, was surprising. Indeed, there are indications that agonist anti-Fas antibodies (Fas is another TNFR family member) need to be oligomerized in order to be active. For example, the CH11 IgM monoclonal antibody directed against human Fas was obtained by immunization of mice with membranes of FS-7 human fibroblasts (27). When an IgG1 recognizing the exact same epitope (mAb ZB4) or a divalent Fab'₂ of CH11 was used, there was no agonist activity (28). A second example of an agonist monoclonal antibody directed against human Fas is APO-1, which was obtained by immunizing mice with plasma membranes of the human SKW 6.4 cell line (29). This antibody is an IgG3. Upon isotype switch, it loses its agonist activity (30), a result that was tentatively explained by the propensity of IgG3 to self-aggregate. As immunoglobulin preparations often contain low amounts of high molecular weight antibody aggregates (31), we wondered whether the agonist activity of anti-EDAR antibodies could be due to aggregates. This was however not the case as monomeric antibodies had a similar specific activity *in vivo* as the total preparation. In addition, a purified Fab'₂ fragment was agonist *in vivo*, whereas the Fab fragment was not. We conclude that divalency is necessary and sufficient for anti-EDAR agonist antibodies to exert their activity.

We have shown previously that the collagen domain of EDA oligomerizes the trimeric TNF-homology domain of EDA1 into higher order structures with concomitant gain of activity (13). Similarly, Fc-EDA1 that assembles as a hexamer (containing two EDA1 trimers) is a highly active molecule. One interpretation is that multiple EDAR molecules must be recruited within the same complex in order to deliver robust intracellular signals, but this is in apparent contradiction with the observation that divalent antibodies are good agonists. A first hypothesis to reconcile these observations is that EDAR may

pre-exist as inactive complexes before ligand binding, as previously shown for Fas (32). Binding of a ligand may a) change the conformation of the complex to render it signaling competent and b) bring together two such complexes to initiate signaling. Divalent agonist antibodies may mimic hexavalent ligands by a) inducing the conformational change by binding one receptor in the pre-assembled complex and b) recruiting and activating a second complex on its second arm. In a second hypothesis, binding of the ligand or the antibody at an appropriate site of EDAR is sufficient to render the receptor signaling competent. Assembly of the signaling complex may however be relatively slow and reversible if the agonist detaches prematurely from the receptor. In this model, efficient signaling could be obtained either with divalent reagents with low dissociation constants, or with ligands that compensate relatively high dissociation constants by multivalency. Whatever their mechanism of action, Fc-EDA1 and agonist anti-EDAR antibodies are in practice excellent agonists to cure

animal models of XLHED, including their teeth defects. Because of their long half-life *in vivo*, agonist anti-EDAR antibodies will prove useful reagents for long-term experiments, especially in mice where these mouse antibodies should elicit minimal neutralizing immune responses.

Finally, it is noteworthy that keratoconjunctivitis sicca (dry eye) that affects all untreated EDA-deficient dogs is believed to be caused by decreased tear production. Tear production improved significantly in two of the treated dogs but not in a third one (E237). Nevertheless, none of the dogs treated in this study with agonist anti-EDAR antibody required therapy for dry eye or any other ocular disorders. These findings suggest that decreased tear production is not the only factor causing dry eyes, but that other structures such as Meibomian glands that lubricate the eye, or the composition of the lipids therein, also play an important role.

REFERENCES

1. Aggarwal, B. B. (2003) *Nat Rev Immunol* **3**, 745-756
2. Mikkola, M. L. (2008) *Cytokine Growth Factor Rev* **19**, 219-230
3. Yan, M., Wang, L. C., Hymowitz, S. G., Schilbach, S., Lee, J., Goddard, A., de Vos, A. M., Gao, W. Q., and Dixit, V. M. (2000) *Science* **290**, 523-527
4. Headon, D. J., Emmal, S. A., Ferguson, B. M., Tucker, A. S., Justice, M. J., Sharpe, P. T., Zonana, J., and Overbeek, P. A. (2001) *Nature* **414**, 913-916
5. Headon, D. J., and Overbeek, P. A. (1999) *Nat Genet* **22**, 370-374
6. Monreal, A. W., Zonana, J., and Ferguson, B. (1998) *Am J Hum Genet* **63**, 380-389
7. Newton, K., French, D. M., Yan, M., Frantz, G. D., and Dixit, V. M. (2004) *Mol Cell Biol* **24**, 1608-1613
8. Srivastava, A. K., Pispá, J., Hartung, A. J., Du, Y., Ezer, S., Jenks, T., Shimada, T., Pekkanen, M., Mikkola, M. L., Ko, M. S., Thesleff, I., Kere, J., and Schlessinger, D. (1997) *Proc Natl Acad Sci U S A* **94**, 13069-13074
9. Nakata, M., Koshihara, H., Eto, K., and Nance, W. E. (1980) *Am J Hum Genet* **32**, 908-919
10. Pinheiro, M., and Freire-Maia, N. (1979) *Am J Med Genet* **4**, 113-122
11. Zankl, A., Addor, M. C., Cousin, P., Gaide, A. C., Gudinchet, F., and Schorderet, D. F. (2001) *Eur J Pediatr* **160**, 296-299
12. Schneider, P., Street, S. L., Gaide, O., Hertig, S., Tardivel, A., Tschopp, J., Runkel, L., Alevizopoulos, K., Ferguson, B. M., and Zonana, J. (2001) *J Biol Chem* **276**, 18819-18827
13. Swee, L. K., Ingold-Salamin, K., Tardivel, A., Willen, L., Gaide, O., Favre, M., Demotz, S., Mikkola, M., and Schneider, P. (2009) *J Biol Chem* **284**, 27567-27576
14. Mues, G., Tardivel, A., Willen, L., Kapadia, H., Seaman, R., Frazier-Bowers, S., Schneider, P., and D'Souza, R. N. (2010) *Eur J Hum Genet* **18**, 19-25
15. Mustonen, T., Pispá, J., Mikkola, M. L., Pummila, M., Kangas, A. T., Pakkasjarvi, L., Jaatinen, R., and Thesleff, I. (2003) *Dev Biol* **259**, 123-136

16. Cui, C. Y., Durmowicz, M., Ottolenghi, C., Hashimoto, T., Griggs, B., Srivastava, A. K., and Schlessinger, D. (2003) *Hum Mol Genet* **12**, 2931-2940
17. Casal, M. L., Lewis, J. R., Mauldin, E. A., Tardivel, A., Ingold, K., Favre, M., Paradies, F., Demotz, S., Gaide, O., and Schneider, P. (2007) *Am J Hum Genet* **81**, 1050-1056
18. Gaide, O., and Schneider, P. (2003) *Nat Med* **9**, 614-618
19. Casal, M. L., Scheidt, J. L., Rhodes, J. L., Henthorn, P. S., and Werner, P. (2005) *Mamm Genome* **16**, 524-531
20. Bossen, C., Ingold, K., Tardivel, A., Bodmer, J. L., Gaide, O., Hertig, S., Ambrose, C., Tschopp, J., and Schneider, P. (2006) *J Biol Chem* **281**, 13964-13971
21. Schneider, P. (2000) *Meth. Enzymol.* **322**, 325-345
22. Wang, Z., Raifu, M., Howard, M., Smith, L., Hansen, D., Goldsby, R., and Ratner, D. (2000) *J Immunol Methods* **233**, 167-177
23. Schneider, P., Holler, N., Bodmer, J. L., Hahne, M., Frei, K., Fontana, A., and Tschopp, J. (1998) *J Exp Med* **187**, 1205-1213
24. Rawlins, E. L., and Hogan, B. L. (2005) *Dev Dyn* **233**, 1378-1385
25. Mauldin, E. A., Gaide, O., Schneider, P., and Casal, M. L. (2009) *Am J Med Genet A* **149A**, 2045-2049
26. Shawlot, W., Siciliano, M. J., Stallings, R. L., and Overbeek, P. A. (1989) *Mol Biol Med* **6**, 299-307
27. Yonehara, S., Ishii, A., and Yonehara, M. (1989) *J Exp Med* **169**, 1747-1756
28. Fadeel, B., Thorpe, C. J., Yonehara, S., and Chiodi, F. (1997) *Int Immunol* **9**, 201-209.
29. Trauth, B. C., Klas, C., Peters, A. M., Matzku, S., Moller, P., Falk, W., Debatin, K. M., and Krammer, P. H. (1989) *Science* **245**, 301-305
30. Dhein, J., Daniel, P. T., Trauth, B. C., Oehm, A., Moller, P., and Krammer, P. H. (1992) *J Immunol* **149**, 3166-3173
31. Ahrer, K., Buchacher, A., Iberer, G., Josic, D., and Jungbauer, A. (2003) *J Chromatogr A* **1009**, 89-96
32. Siegel, R. M., Frederiksen, J. K., Zacharias, D. A., Chan, F. K., Johnson, M., Lynch, D., Tsien, R. Y., and Lenardo, M. J. (2000) *Science* **288**, 2354-2357.

Acknowledgments - We thank Christophe Maier (Edimer Biotech, Epalinges) for his invaluable input in the creation of Edimer, Jeff Behrens and Neil Kirby for their motivating discussions, support and for the gift of Fc-EDA, Stéphane Germain for his assistance in early phases of mice work, Olivier Donzé for expert help in the generation of the antibodies, John Lewis for dental pictures of the dogs, veterinary technicians and students of the University of Pennsylvania for the expert care of the dogs, and Jürg Tschopp for his continuous support and helpful discussions. This work was supported by grants from the Swiss National Science Foundation (to PS) and the NIH (RR02512, to MLC). Anti-EDAR sequences have been deposited in GenBank under accession numbers JN099705 to JN099733.

Conflicts of interest – PS, MC, OG and SD are shareholders of EdimerPharma. Other authors declare no competing financial interests.

FIGURE LEGENDS

Fig. 1. Purity of protein-G purified anti-EDAR monoclonal antibodies.

Anti-EDAR monoclonal antibodies were purified by protein G affinity chromatography from culture supernatants in serum-free medium (antibodies 1-4, 6-10, 12-14) or in serum-containing medium (antibodies 5, 11 and 15).

Panel A. SDS-PAGE analysis and Coomassie blue staining of 10 µg antibody per lane under reducing conditions. Migration positions of molecular weight standards (in kDa) are shown.

Panel B. Native gel electrophoresis of 4 µg anti-EDAR antibodies per lane, stained with amidoblack.

Fig. 2. Epitope mapping of anti-EDAR monoclonal antibodies.

Panel A. Schematic linear representation of human EDAR showing the position of cystein residues (thin horizontal lines), of the putative N-linked glycosylation site (thick horizontal line, N) and of the six structural modules (rectangles with rounded corners) composing the three cystein-rich domains (CRD1, CRD2, CRD3). The transmembrane domain (TMD), signal peptide (Leader), stalk and intracellular domain (ID) are also shown. Amino acid numbers at the junctions of interest are indicated. The arrow indicates the predicted cleavage site of the signal peptide. The scheme is drawn to scale, except for the intracellular domain.

Panel B. The indicated EDAR-Fc constructs or BCMA-Fc control were captured in an ELISA plate and revealed with the indicated anti-EDAR antibodies, or with an anti-human IgG to control efficient capture of the various EDAR-Fc proteins, or with Flag-EDA1 or Flag-BAFF as controls.

Panel C. Bovine serum albumin (B; BSA, 2 μ g), hEDAR-Fc (E, 20 ng) and hFas-Fc (F, 20 ng), were resolved by SDS-PAGE under reducing or non-reducing conditions, transferred onto nitrocellulose and probed with anti-EDAR 1 to 15.

Fig. 3. Cross-species specificity of anti-EDAR antibodies.

Receptors fused to the GPI anchor of TRAILR3 were expressed in 293T cells together with an EGFP tracer (*x*-axis) and stained with Fc-EDA1, Fc-EDA2 or with anti-EDAR antibodies (*y*-axis). Receptor expression was confirmed by staining with an antibody directed against the C-terminal portion of TRAILR3 present in all constructs (mAb572). Both scattergram axes show fluorescence intensity on a logarithmic scale (10^0 – 10^4).

Fig. 4. Generation and binding characteristics of anti-EDAR Fab fragments.

Panel A. Superdex-200 gel permeation chromatography elution profiles of intact and ficin-digested anti-EDAR antibodies. In the digested antibodies, Fc fragments and undigested antibodies were first removed by chromatography on Protein A. Peak identities are indicated.

Panel B. Fab fragments at the indicated concentrations were analyzed by surface plasmon resonance onto immobilized hEDAR-Fc. Fab solutions were applied for 90 sec, and subsequently washed with buffer. Results for 3 antibodies with distinct binding characteristics are shown.

Fig. 5. *In vitro* activity of anti-EDAR antibodies in a surrogate reporter assay.

Panel A. Anti-EDAR antibodies and Fc-EDA1 were tested for their capacity to induce apoptosis of mEDAR:Fas-expressing Jurkat cells. After overnight culture, cell viability was determined by the PMS/MTS cell viability assay. EC_{50} are indicated as dotted lines. Anti-EDAR antibody number (or Fc-EDA1) for each curve is indicated to the right of each panel.

Panel B. *Idem*, except that hEDAR:Fas expressing cells were used.

Fig. 6. Therapeutic doses of the anti-EDAR antibodies in newborn *Tabby* mice.

Newborn *Tabby* mice were injected intra-peritoneally during the first 24 h of life with graded doses of anti-EDAR antibodies, an irrelevant mouse IgG1 (Aprily 5) or Fc-EDA1. Four to six weeks later (antibody 2, 3 and 4) or 3 weeks later (antibodies 1, 4 to 14 and Aprily5), hair density on the tail was scored according to the criteria shown in the insert. The anti-EDAR antibody 1 used in this experiment was the monomer peak obtained by gel filtration (see Fig. 4).

Fig. 7. An anti-EDAR antibody reverts many ectodermal dysplasia phenotypes in EDA-deficient mice.

Pregnant *Tabby* mice were treated iv at day 13 and 20 (E13/E20) of gestation with anti-EDAR antibody 3 at 16 mg/kg. Offspring were analyzed at 6 months of age. Age-matched wild-type and EDA-deficient *Tabby* mice were similarly analyzed for comparison.

Panel A. Tail phenotype. Panel B. Transversal sections of tail skin showing the presence of hair follicles, stained with hematoxylin and eosin. Panel C. Starch iodine sweat tests. Panel D. Sections of foot pads showing the presence of glandular structures of sweat glands (arrowheads), stained with hematoxylin and

eosin. Panel E. Top view of the retro-auricular region showing the presence of hair behind the ears. Panel F. Sections of the trachea stained with Alcian blue to reveal mucus-secreting glands (arrowheads). Panel G. Eye phenotype showing reversion of the thickened eyelid margin and narrow eyelid opening. Panels H, I. Pictures of the jaw carrying the upper and lower molars. Antibody treated and wild type jaws carry larger teeth with a normal pattern of cusps on their surfaces.

Fig. 8. An anti-EDAR antibody ameliorates dentition and presence of glands in EDA-deficient dogs. An EDA-deficient dog was treated at day 2 of live with a single dose of anti-EDAR (antibody 3) at 10 mg/kg, and analyzed 1.6 years later in comparison with a wild type and with an affected dog. Panels A and B: Front and side views of the jaws. Panels C and D: Hematoxylin and eosin-stained tissue sections of the trachea and bronchi. Glandular tissues are indicated with arrowheads.

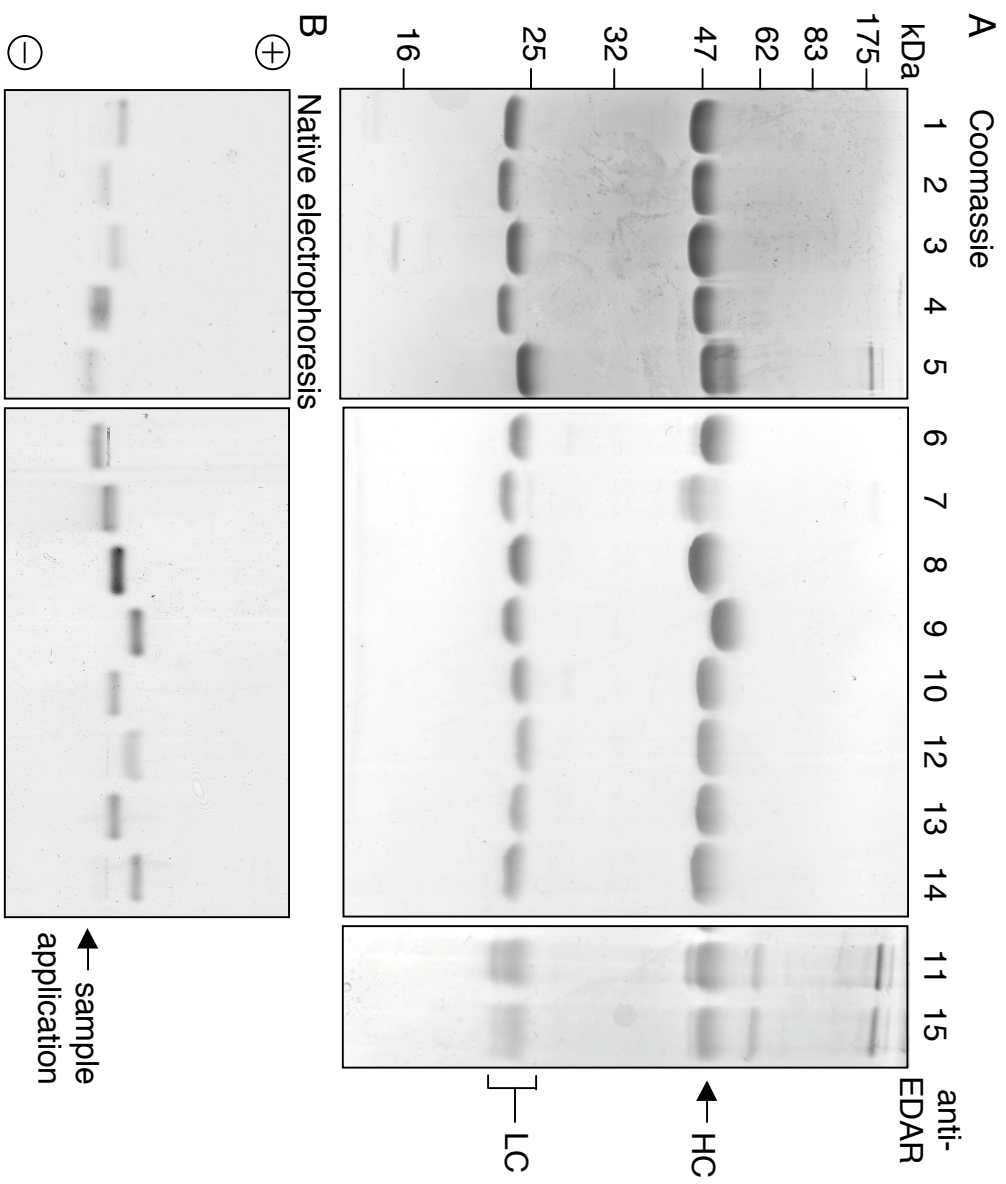
Table 1. Characteristics of anti-EDAR monoclonal antibodies.

Anti-EDAR	IGHV gene	IGLV gene	Anti-Gen	Iso-type	Epi-tope	ka M ⁻¹ s ⁻¹ * 10 ⁻⁵	kd s ⁻¹ * 10 ⁴	KD nM	EC50 tail hair mg/kg	EC50 mEDAR :Fas ng/ml	EC50 hEDAR: Fas ng/ml
1	5-17	10-96	hu	IgG1	I + II	6.79	3.69	0.54	0.125	10	200
2	1-69	1-117	hu	IgG1	I + II	13.2	13.3	1.00	0.42	>4000	>4000
3	5-17	10-96	hu	IgG1	I + II	ND	ND	ND	0.18	30	100
4	ND	1-117	hu	IgG1	I + II	4.50	13.6	3.01	0.7	>4000	>4000
5	2-2	4-91	hu	IgG2b	I	ND	ND	ND	0.25	>4000	>4000
6	1S135	1-110	hu	IgG2a	I	3.81	6.02	1.58	0.25	>4000	>4000
7	7-3	4-577	hu	IgG1	I + II	2.92	96.6	33.1	0.3	>4000	>4000
8	5-17	10-96	mu	IgG1	I + II	8.12	3.86	0.48	0.5	100	>4000
9	1-63	1-117	mu	IgG1	I+II+III	1.89	8.44	4.46	0.42	>4000	>4000
10	1-39	4-55	hu	IgG1	I + II	0.35	2.38	6.78	0.125	10	50
11	1-39	10-94	hu	IgG1	I + II	ND	ND	ND	3.3	>4000	>4000
12	1-14	17-12	mu	IgG1	I	0.41	6.66	16.3	0.35	10	5
13	1S135	1-110	hu	IgG1	I	1.83	18.7	10.2	0.42	>4000	>4000
14	1-42	10-94	mu	IgG1	I + II	1.90	74.8	39.3	0.3	>4000	>4000
15	1-63	12-44	hu	IgG1	I + II	ND	ND	ND	ND	ND	ND

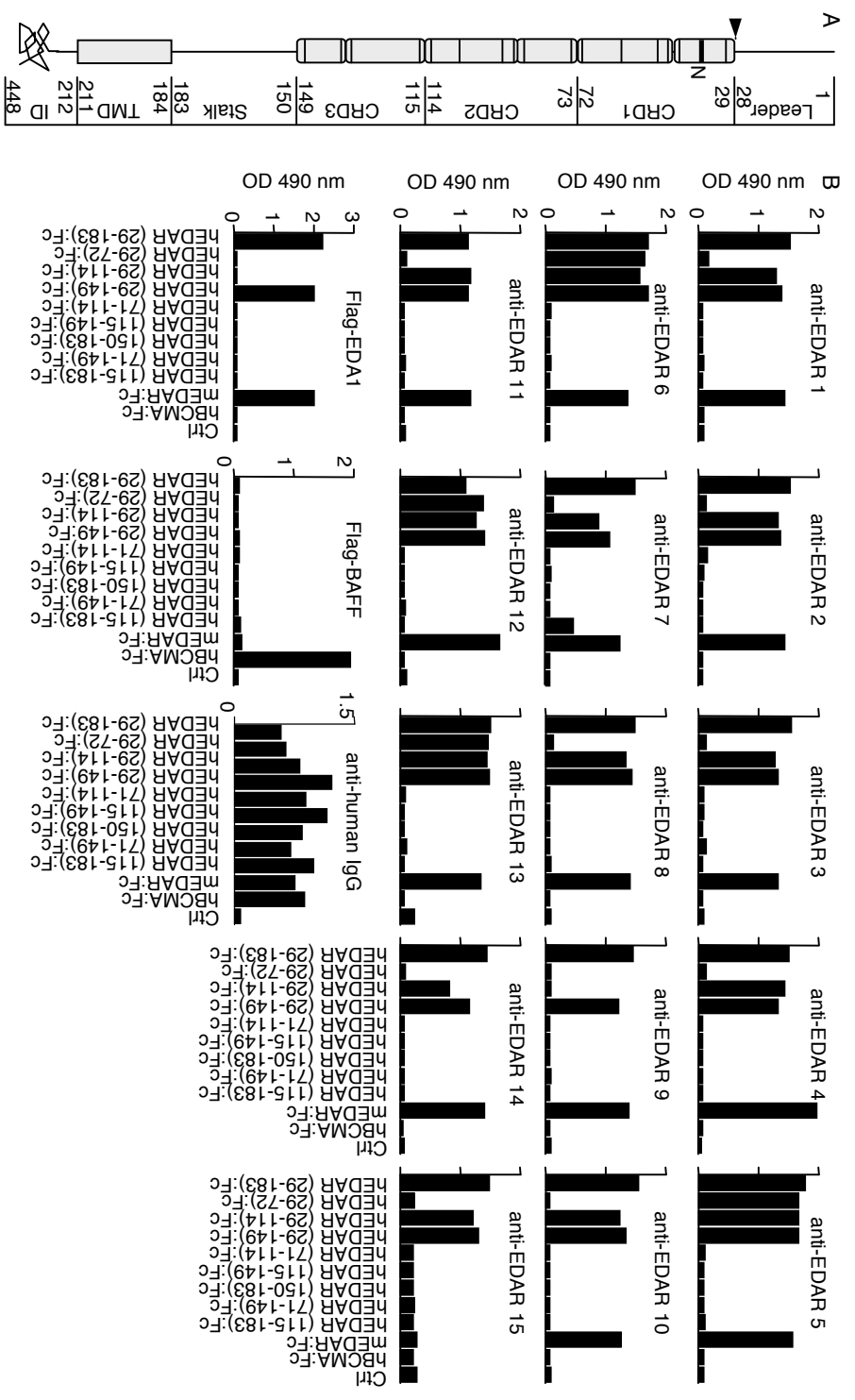
IGHV, IGLV: immunoglobulin heavy and light chains variable region genes likely used in the antibody.
 hu: human EDAR-Fc. mu: Mouse EDAR-Fc. I + II: EDAR-Fc containing CRD1 and CRD2 of human EDAR. I: EDAR-Fc containing CRD1 only. Full: EDAR-Fc containing the full extracellular domain of EDAR. ka: association constant. kd: dissociation constant. KD: affinity of monomeric Fab to EDAR-Fc. EC50 tail hair: dose of antibody required to get half maximal tail hair reversion score when administered ip in newborn *Tabby* mice. EC50 mEDAR:Fas or hEDAR:Fas: dose of antibody required to kill half of the EDAR:Fas expressing Jurkat cells.

Table 2. Summary of clinical and pathological findings in untreated XLHED dogs and XHLED dogs treated with anti-EDAR antibody 3. *day 14 or day 2 of life.

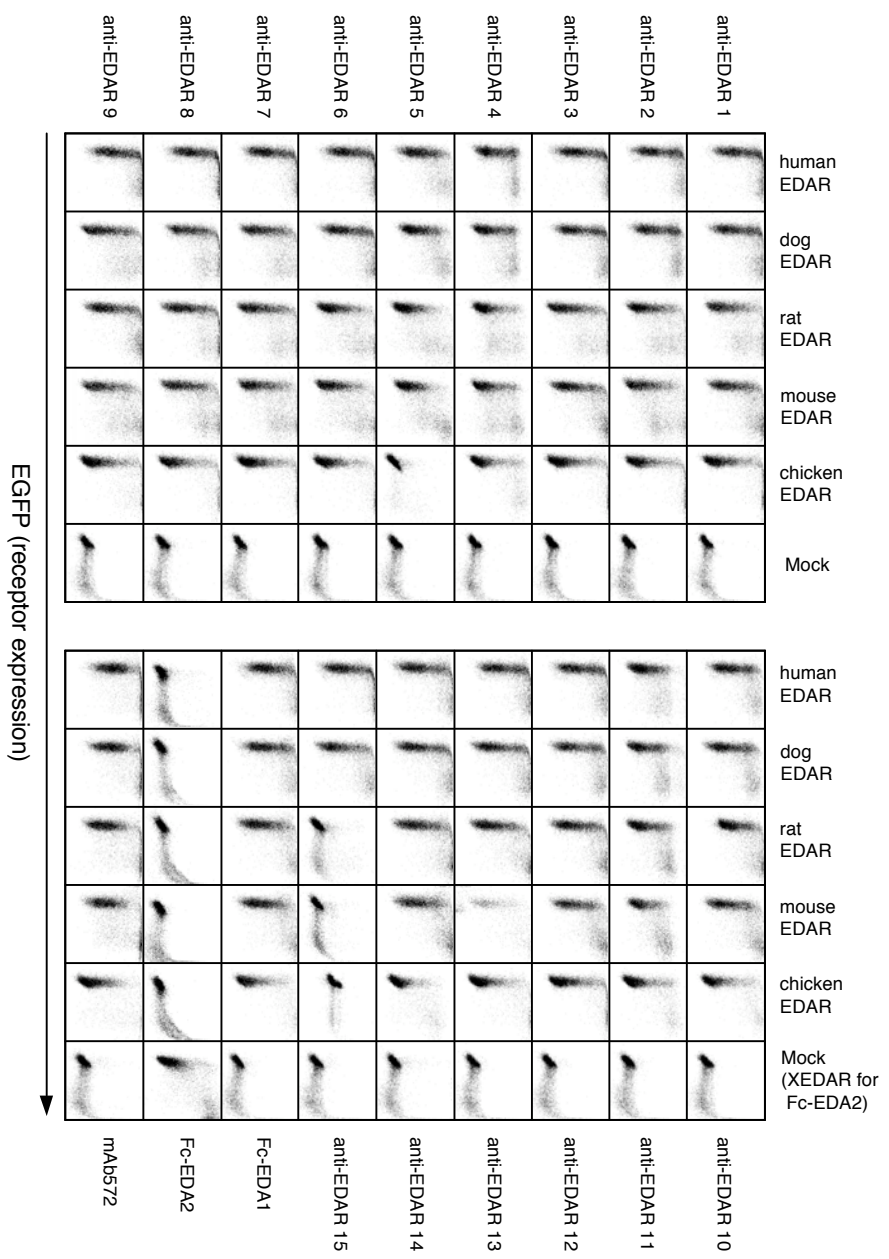
Dog #	Treatment protocol	Age at necropsy	Appearance of teeth (number)	Tracheal glands	Bronchial glands	Esophageal glands	Tear production
Wildtype (n=5)		1-3 yrs	Normal (41.6±0.9)	+++	+++	+++	97 ± 14%
XLHED (n=6)		1-3 yrs	Abnormal (18.0 ± 2.9)	None	None	None	68 ± 20%
E237	10 mg/kg on day 2*	1.7 yrs	Greatly improved (40)	+++	+++	+++	70.0 ± 4.1%
E241	10 mg/kg on day 2*	1.6 yrs	Greatly improved (41)	++	+	++	90.0 ± 7.1%
E222	7 mg/kg on day 14*	2.4 yrs	Improved (30)	+	-	+	80.0 ± 27.1%



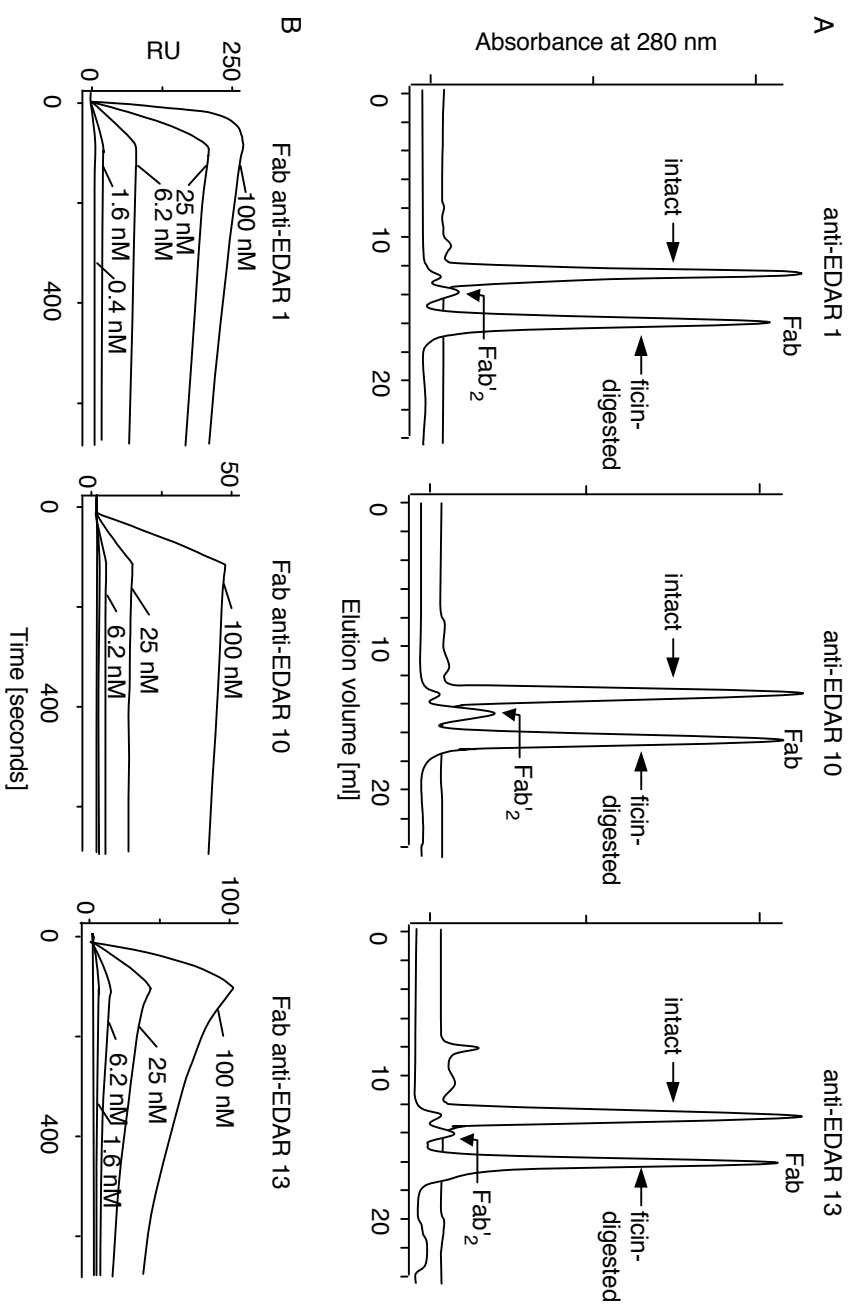
Kowalczyk et al. Figure 1



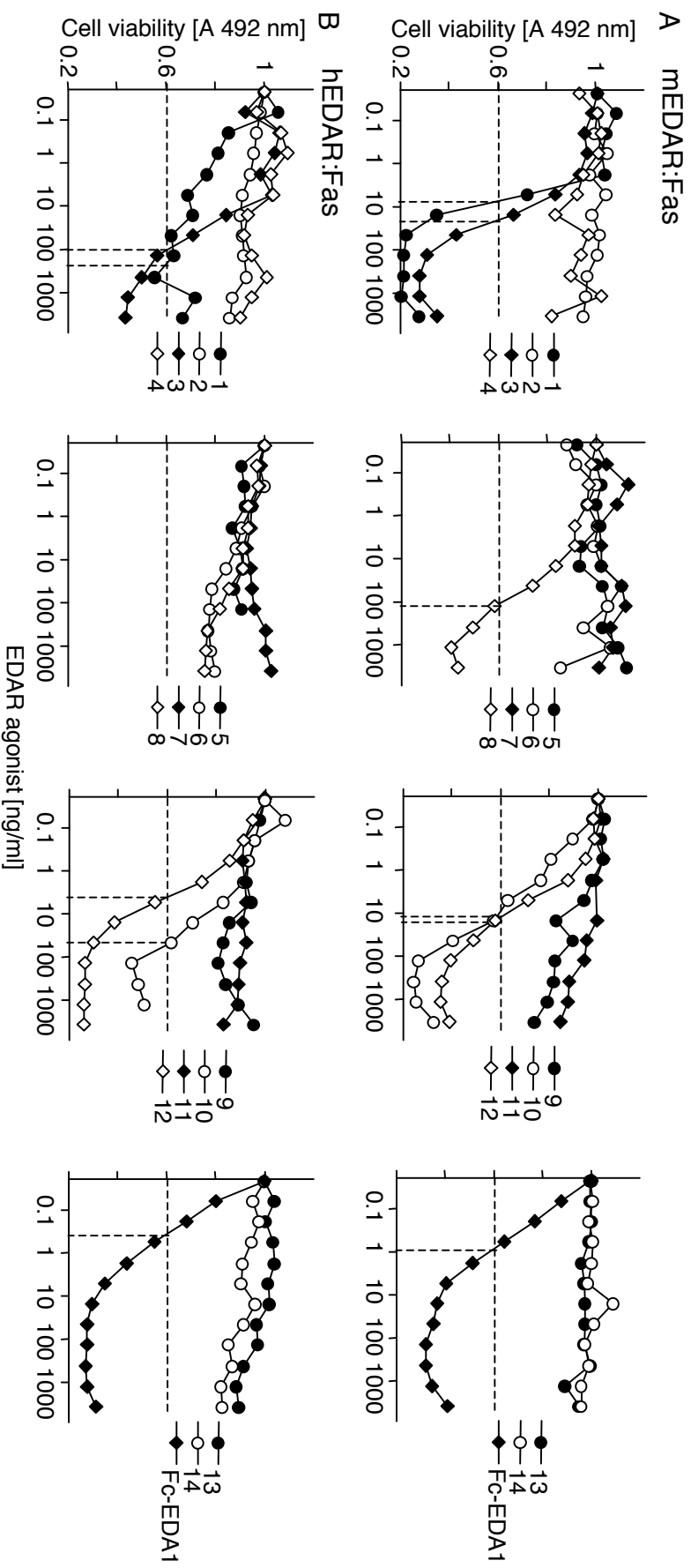
Kowalczyk et al. Figure 2



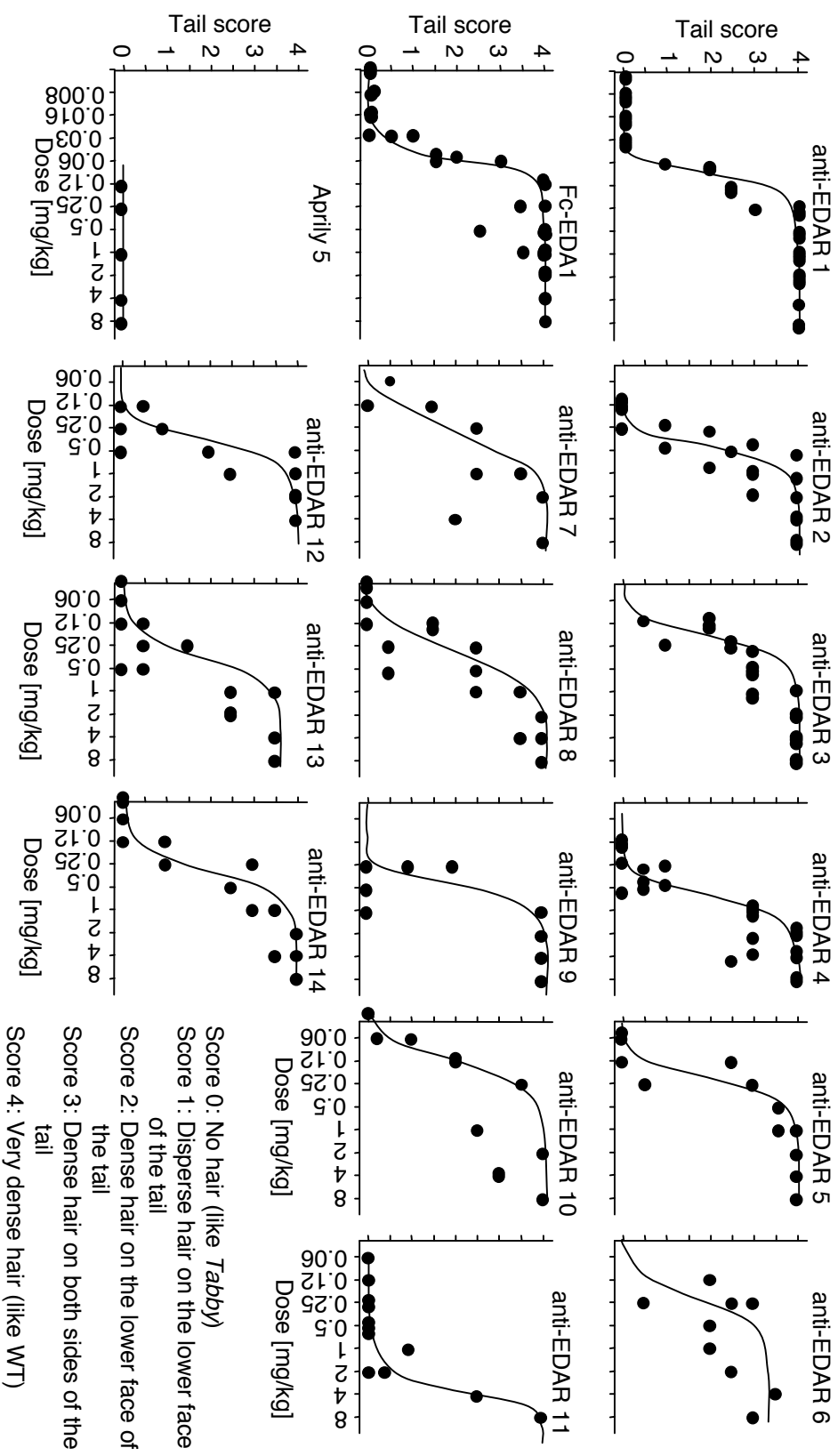
Kowalczyk et al. Figure 3



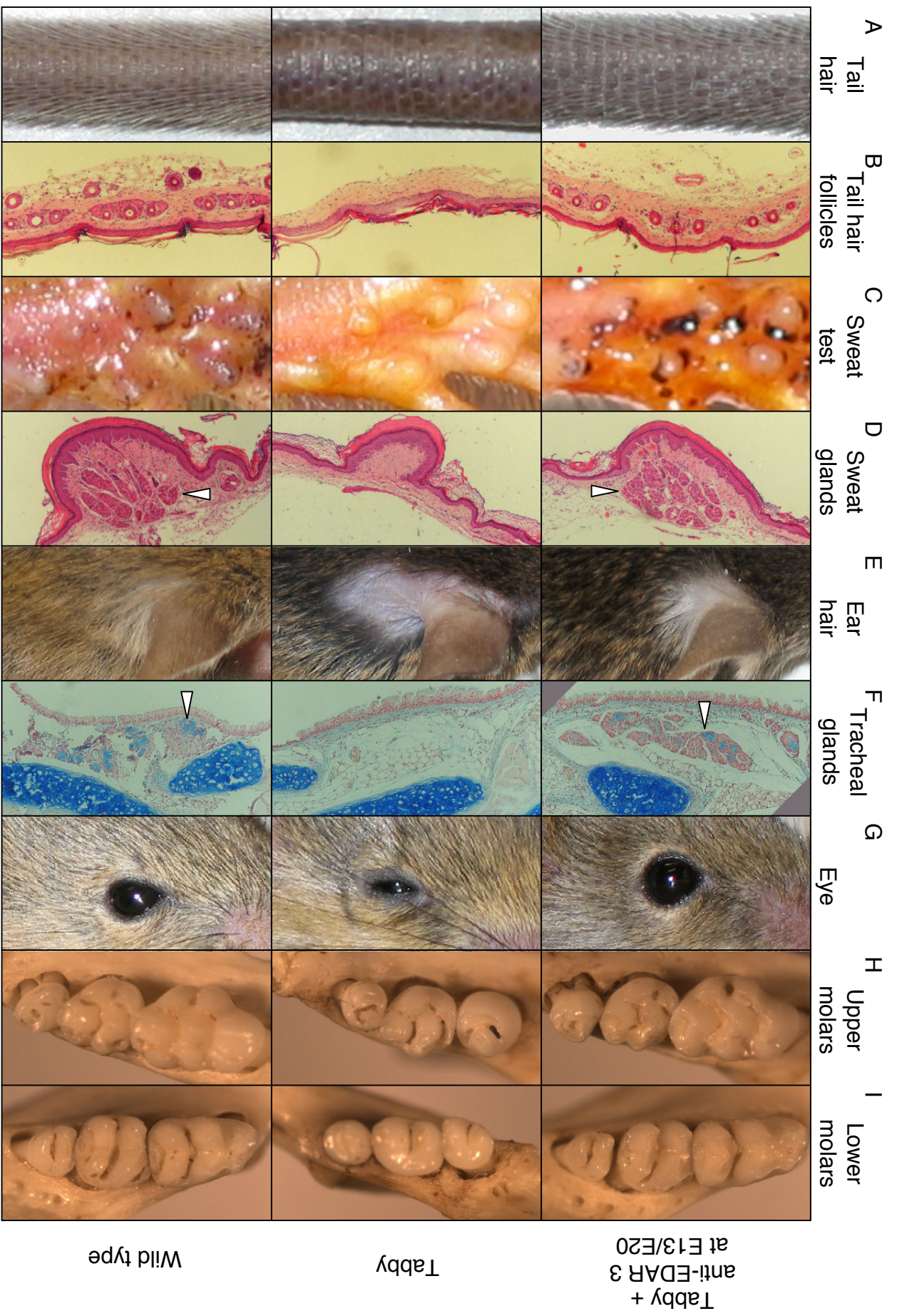
Kowalczyk et al. Figure 4



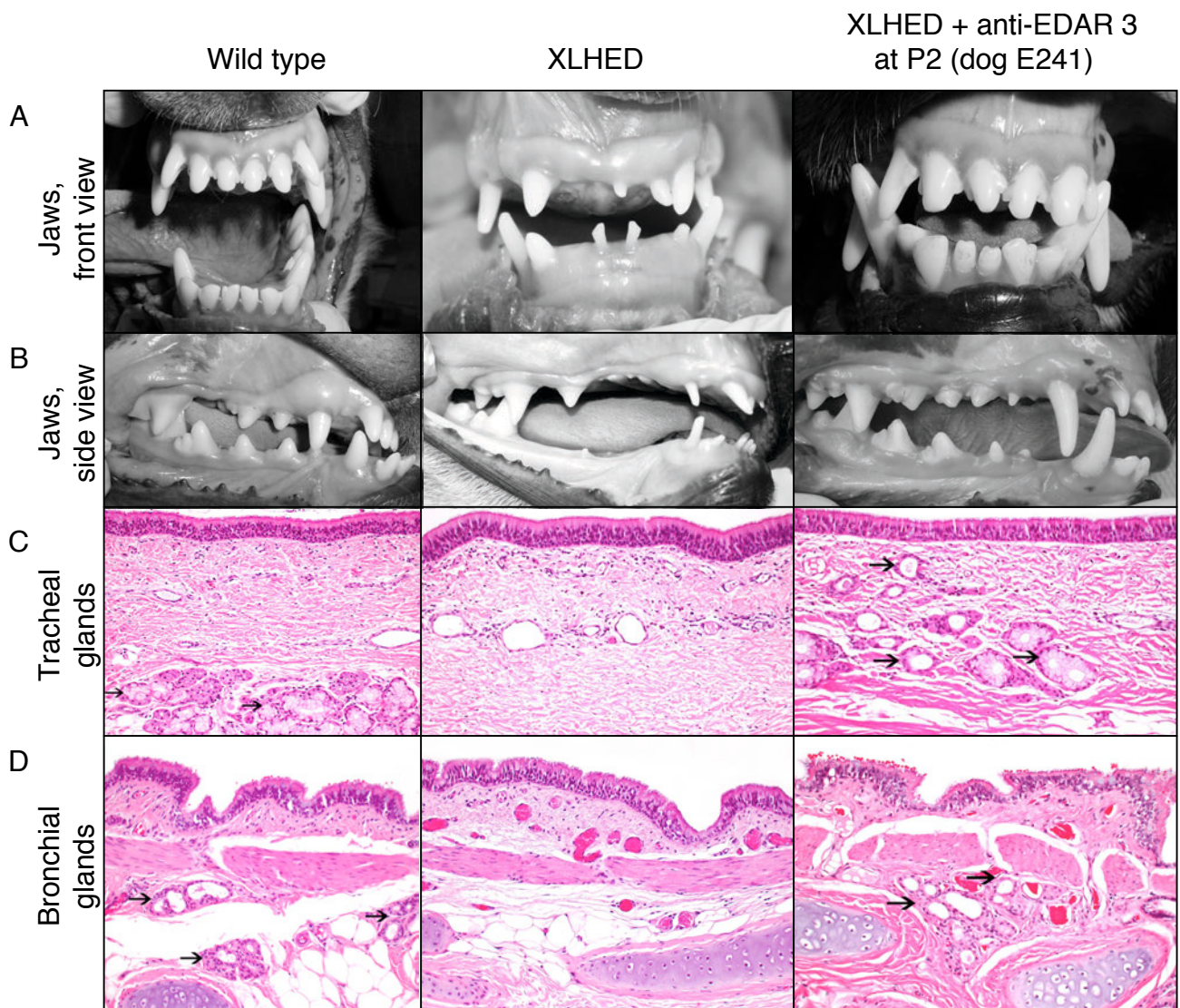
Kowalczyk et al. Figure 5



Kowalczyk et al. Figure 6



Kowalczyk et al. Figure 7



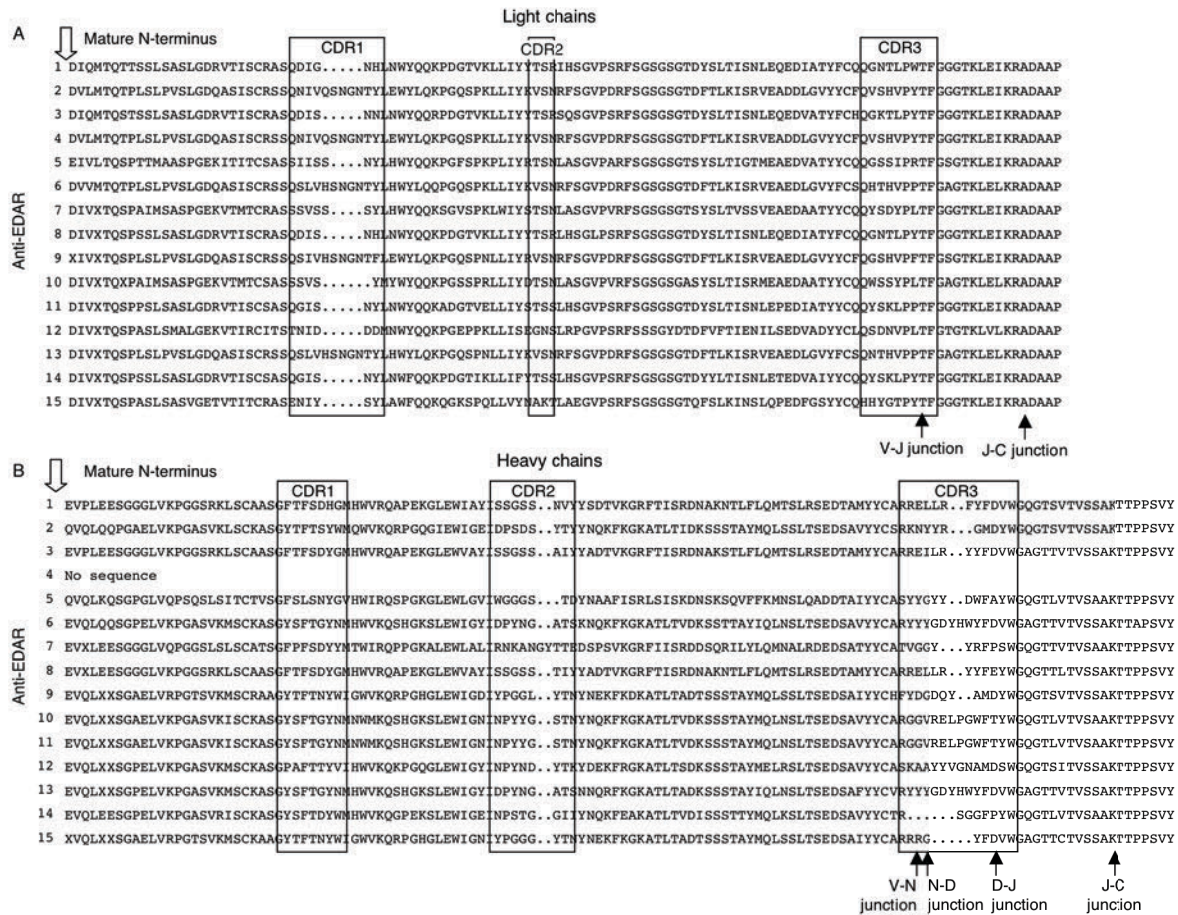
Kowalczyk et al. Figure 8

Online Supplemental Material

Plasmid	Designation	Protein encoded	Vector	Figure
ps515	EGFP	Enhanced green fluorescent protein	PCR3	3
ps1938	Fc-EDA1	Signal-hIgG1 (aa 245-470)-hEDA1 (aa 238-391)	PCR3	3, 5, 6
ps1377	pMSCV-puro	Modified pMSCV-puro (Clonetech) with HindIII-BglII-EcoRI-NotI-XhoI-HpaI-ApaI cloning sites	pMSCV	
ps2199	hEDAR:Fas	hEDAR (aa 1-183)-VD-hFas (aa 169-335)	ps1377	5B
ps2260	mEDAR:Fas	mEDAR (aa 1-183)-VD-hFas (aa 169-335)	ps1377	5A
ps1235	Fc-EDA2	Signal-LD-hIgG1 (aa 245-470)-hEDA2 (aa 245-389)	PCR3	3
ps1431	hEDAR-GPI	hEDAR (aa 1-183)-VD-hTRAILR3 (aa 157-259)	PCR3	3
ps2783	dogEDAR-GPI	dogEDAR (aa 1-183)-VD-hTRAILR3 (aa 157-259)	PCR3	3
ps2765	ratEDAR-GPI	ratEDAR (aa 1-179)-VD-hTRAILR3 (aa 157-259)	PCR3	3
ps1765	mEDAR-GPI	mEDAR (aa 1-183)-VD-hTRAILR3 (aa 157-259)	PCR3	3
ps2290	chEDAR-GPI	chEDAR (aa 1-183)-VD-hTRAILR3 (aa 157-259)	PCR3	3
ps548	Flag-EDA1	Signal-Flag-GPGQVQLQVD-mEDA1 (aa 245-391)	PCR3	2
ps336	Flag-BAFF	Signal-Flag-GPGQVQLQ-hBAFF (aa 137-285)	PCR3	2
ps930	hEDAR-Fc	hEDAR (aa 1-183)-VD-hIgG1 (aa 245-470)	PCR3	2
ps2887	hEDAR (CRD1+2+3)-Fc	hEDAR (aa 1-149)-VD-hIgG1 (aa 245-470)	PCR3	2
ps2484	hEDAR (CDR1+2)-Fc	hEDAR (aa 1-114)-VD-hIgG1 (aa 245-470)	PCR3	2
ps2481	hEDAR(CRD1)-Fc	hEDAR (aa 1-72)-VD-hIgG1 (aa 245-470)	PCR3	2
ps2482	hEDAR (CRD2)-Fc	Signal-LE-hEDAR (aa 71-114)-VD-hIgG1 (aa 245-470)	PCR3	2
ps2524	hEDAR(CRD3)-Fc	Signal-LE-hEDAR (aa 115-149)-VD-hIgG1 (aa 245-470)	PCR3	2
ps2515	hEDAR(CRD2+3)-Fc	Signal-LE-hEDAR (aa 71-149)-VD-hIgG1 (aa 245-470)	PCR3	2
ps2508	hEDAR(CRD3+stalk)-Fc	Signal-LE-hEDAR (aa 115-183)-VD-hIgG1 (aa 245-470)	PCR3	2
ps2509	hEDAR(stalk)-Fc	Signal-LE-hEDAR (aa 150-183)-VD-hIgG1 (aa 245-470)	PCR3	2
ps815	mEDAR-Fc	mEDAR (aa 1-183)-VD-hIgG1 (aa 245-470)	PCR3	2
ps229	hFas-Fc	hFas (aa1-170)-VDhIgG1 (aa 245-470)	PCR3	2

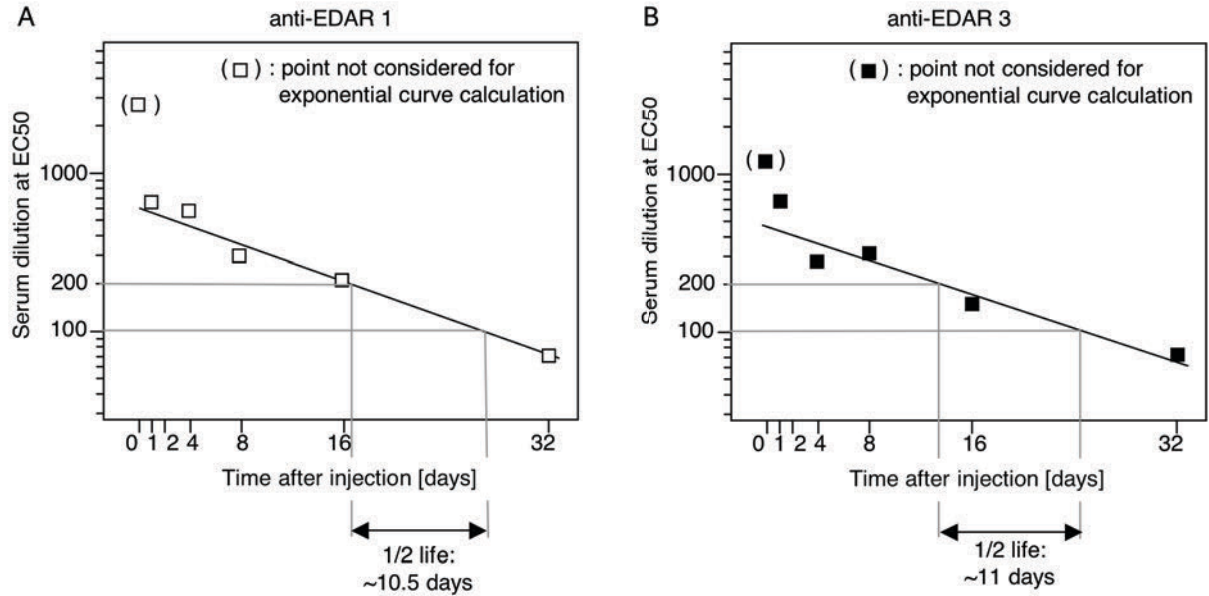
Supplemental Figure 1. List of plasmids used in the study.

Amino acids are indicated with the one letter code or, for large stretches of sequence, by a written description. Signal (signal peptide of haemagglutinin: MAIIYLILLFTAVRG |); Flag (DYKDDDDK); hEDA1, hEDA2 (SwissProt accession number Q92838); human, dog, rat, mouse, chicken EDAR (SwissProt accession numbers Q9UNEO, E2RA80, D3ZGP2, Q9R187 and Q5EFZ7); hFc (IgG1 encoded by GenBank accession number BC018747 or aa105-330 of SwissProt accession number P01857); hFas (SwissProt accession number P25445); Ig signal (Signal peptide of mouse Ig, heavy chain: MNFGFSLIFLVLVLKGVQC | EVKLV). The " | " indicate predicted proteolytic cleavage sites by signal peptidase. Sequences of interest were cloned into the mammalian expression vector PCR3 (Invitrogen) or into the retroviral expression vector pMSCV (Clonetech). Note that ps2765 and ps2783 were obtained by point mutations of the mouse and human sequences, respectively, and therefore are rat and dog sequences at the amino acid level only.



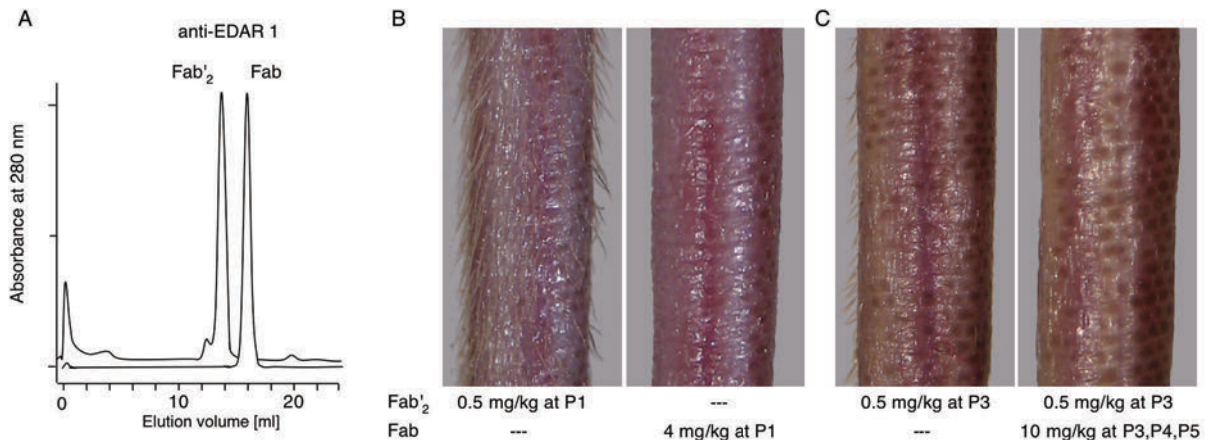
Supplemental Figure 2: **Amino acid sequences of light and heavy chains variable regions of anti-EDAR monoclonal antibodies.**

Sequences start at the mature N-terminus. Complementarity determining regions (CDRs) are highlighted in boxes. Putative junctions of the protein sections encoded by the V, D and J genes, or by randomly added nucleotides (N) are indicated. The junction with the constant region (C) is also shown. Note that the light chains of anti-EDAR antibodies 2 and 4 are identical, and the heavy chains of anti-EDAR antibodies 10 and 11 are identical. Anti-EDAR antibodies 1, 3 and 8 have similar heavy and light chains, most probably originating from the same V_H and V_L genes.



Supplemental Figure 3: **Half-life determination of agonistic anti-EDAR antibodies.**

Wild type mice were intravenously injected with 200 μ l of 1 mg/ml of anti-EDAR 1 or anti-EDAR 3 antibodies. Serum samples were collected after 20 minutes, 1, 2, 8, 16 and 32 days. The concentration of the anti-EDAR mAb was determined by incubating serial dilutions of serum in wells coated with human EDAR-Fc at 1 μ g/ml, followed by horseradish peroxidase-coupled anti-mouse IgG and OPD substrate. For analysis, the serum dilutions giving OD = 1 (considered to represent the EC₅₀) for each time points were plotted as a function of time. An exponential curve was fitted on the series of points except the time point 20 minutes. A half-lives of 10 to 11 days were thus determined for anti-EDAR antibodies 1 and 3.

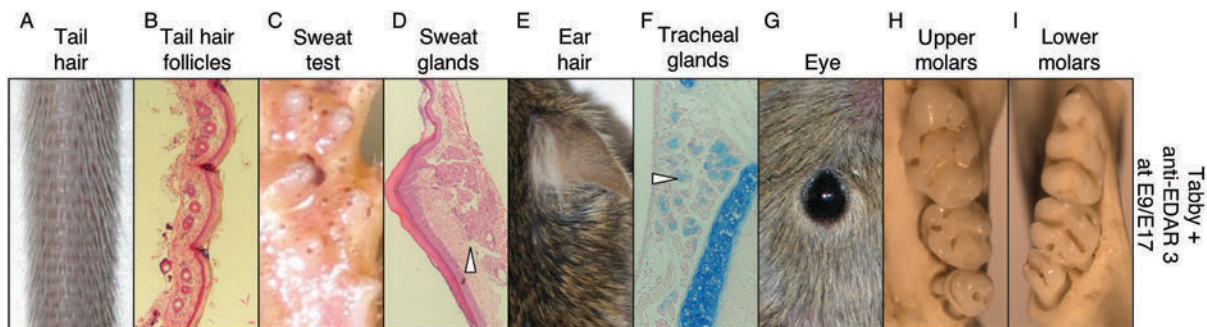


Supplemental Figure 4: An Fab'₂ fragment of an agonist anti-EDAR antibody is active in vivo, whereas a monomeric Fab fragment acts as an inhibitor.

A. Superdex-200 gel permeation chromatography elution profiles of ficin-generated Fab and Fab'₂ fragments of anti-EDAR antibody 1, previously isolated by size exclusion chromatography (see Fig. 4A). Main peaks were collected and used for *in vivo* experiments.

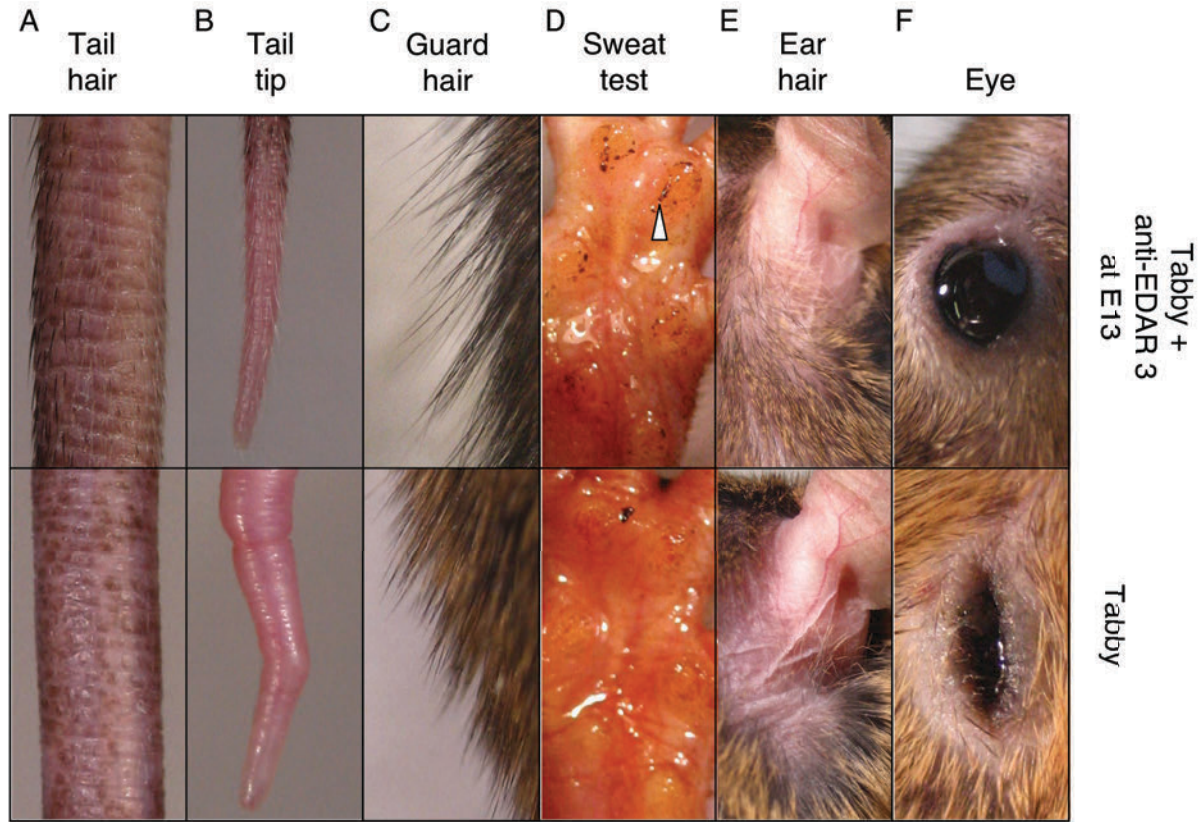
B. The Fab'₂ fragment was injected at 0.5 mg/kg in newborn *Tabby* mice. Tail hair formation was recorded 3 weeks later. Administration of the Fab fragment at 4 mg/kg did not induce tail hair formation (n=3).

C. The Fab'₂ fragment was injected ip at 0.5 mg/kg in 3 days-old *Tabby* pups, which is one of the latest time point at which tail hair formation can still be partially rescued on the ventral side of the tail (on the left of the picture). The Fab fragment was injected at 4 mg/kg 4 h before administration of the Fab'₂ fragment and at 6 mg/kg together with the Fab'₂ fragment. The Fab was then administered again at 10 mg/kg 24 and 48 h later. Co-treatment with the Fab fragment prevented the action of the Fab'₂ fragment.



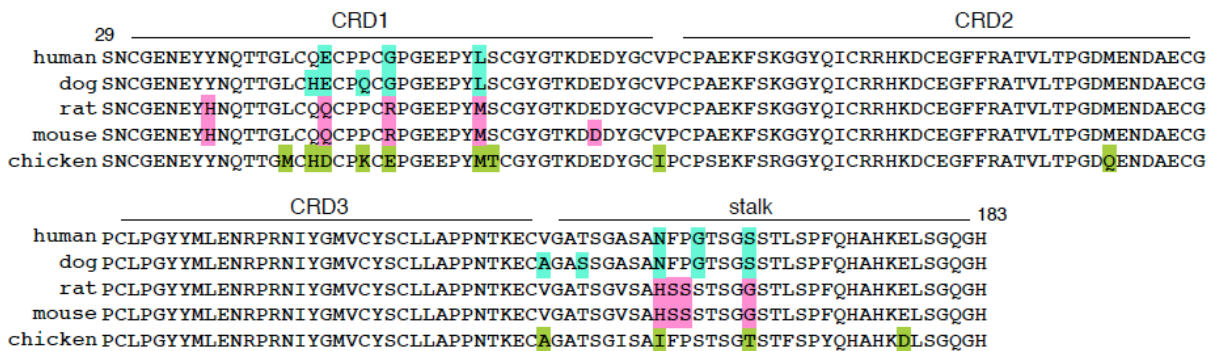
Supplemental Figure 5: An anti-EDAR antibody reverts many ectodermal dysplasia phenotypes in EDA-deficient mice.

A pregnant *Tabby* mouse was treated iv at day 9 and 17 (E9/E17) of gestation with anti-EDAR 3 at 16 mg/kg. Offspring was analyzed at 6 months of age, as described in the legend to Figure 7.



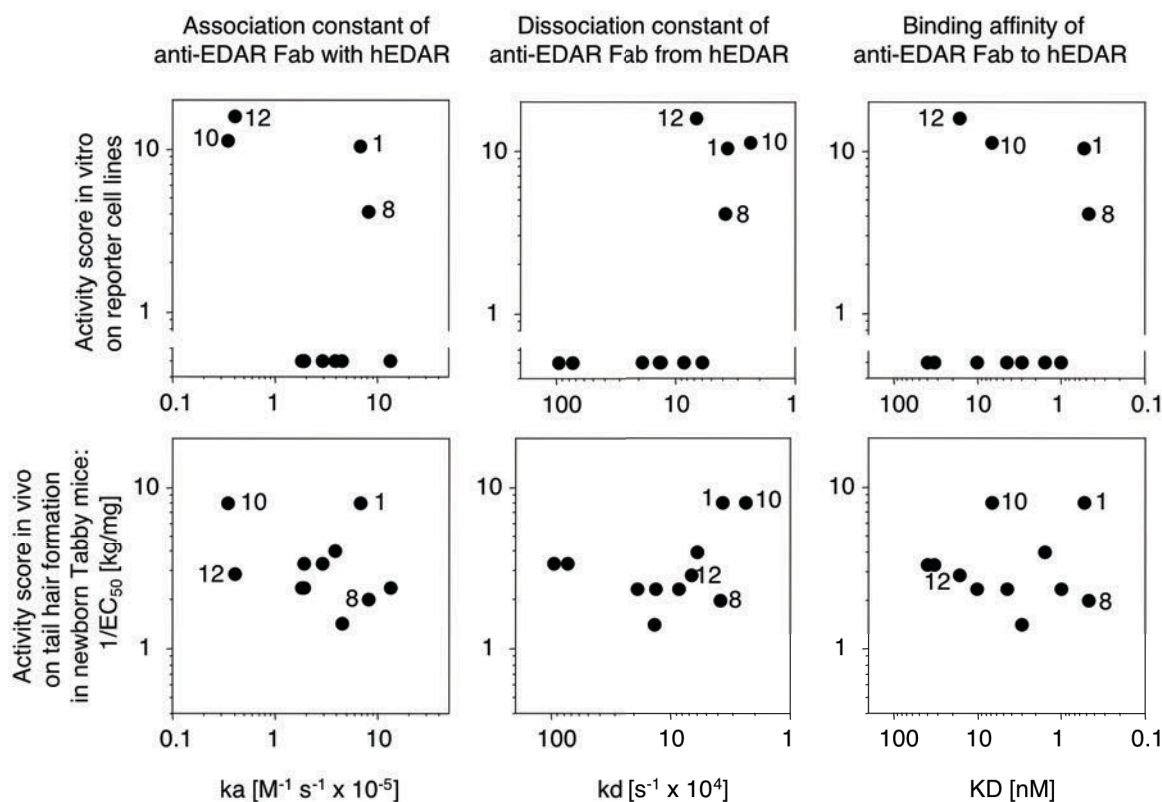
Supplemental Figure 6: **Long-term reversion of ectodermal dysplasia symptoms upon treatment with agonist anti-EDAR antibodies.**

A pregnant *Tabby* mouse was treated iv at day 13 (E13) of gestation with anti-EDAR 3 at 6.5 mg/kg. Offspring and age-matched *Tabby* mouse were analyzed at 26 months of age. A. Tail. B. Tail tip, showing absence of a kink in the treated mouse. C. Back hair, showing the presence of the longer guard hair in the treated mouse. D. Sweat test showing the presence of functional sweat glands in the treated mouse (arrowhead). E. Retro-auricular region. F. Eye.



Supplemental Figure 7: **Amino acid sequence of the mature extracellular domain of EDAR in different species.**

Divergent amino acids are highlighted with colours. The positions of the cystein-rich domains (CRDs) and stalk are indicated.



Supplemental Figure 8: **Correlation between low dissociation constants and agonist activity of anti-EDAR antibodies in an *in vitro* reporter cell line assay.**

Binding characteristics of the agonist anti-EDAR monoclonal antibodies (see Table 1) were plotted against their activity score *in vivo* ($1/EC_{50}$, see Table 1) and their activity score *in vitro*. The activity score *in vitro* was determined as $8 \cdot (1/\log(EC_{50} \text{ hEDAR})) + 5.6 \cdot (1/\log(EC_{50} \text{ mEDAR}))$ (see Table 1 for EC_{50} values). The correction factors 8 and 5.6 were chosen so that the best antibody(ies) in the human or mouse EDAR:Fas assays score(s) 8 points. Antibodies showing agonist activity *in vitro* are identified by their numbers in the graphs.